A Rational Co-Design Approach to the Creation of New Dielectric Polymers with High Energy Density

Gregory M. Treich[1], Mattewos Tefferi[2], Shamima Nasreen[3], Arun Mannodi-Kanakkithodi[4], Zongze Li[2], Rampi Ramprasad[4], Gregory A. Sotzing[1,3] and **Yang Cao[2]**

[1]Polymer Program, University of Connecticut
[2]Department of Electrical and Computer Engineering, University of Connecticut
[3]Department of Chemistry, University of Connecticut
[4]Department of Materials Science and Engineering, University of Connecticut,
Storrs, Connecticut, 06269, United States

ABSTRACT

In order to interface power sources with any electrical load, energy storage and conversion are important components. The ability to store electrical energy is essential in many applications. Dielectric materials with high electric energy density are essential components in modern power electronics such as pulsed power systems and switched mode power supplies. The current state-of-the-art film capacitor is biaxially oriented polypropylene that has a breakdown strength of >730 MV/m and low dielectric loss of <0.0002 at 1 kHz, but suffers a low dielectric constant of 2.2. Novel dielectric materials for film capacitors were synthesized with guidance from a high throughput hierarchal modeling scheme, which involved combinatorial exploration based on density functional theory computations followed by successive screening. As a result, several organic polymers consisting of polythioureas and polyimides have been identified, synthesized, and characterized along with a new class of organometallic polymers. A fundamental understanding of the correlation between materials' molecular and micro structures and their electrical characteristics in the presence of various intrinsic and extrinsic factors is essential to the basic research for the design of new dielectric materials.

Index Terms — **Capacitors, energy storage, polymer film, high dielectric constant, polarization, density functional theory, glass transition.**

1 INTRODUCTION

RAPID advancements in clean and renewable energy technologies calls for better dielectric and electric insulation materials and greater understanding of material phenomena related to electrical energy storage and insulation at high fields [1]. In a modern power system, capacitors are among the most pervasive and least reliable devices used in DC-link of power conversion systems, filtering, power factor correction, and pulsed power systems [1,2]. Biaxially oriented polypropylene (BOPP) based capacitors are presently used at both distribution and transmission voltages for compensation in the DC-link filters of medium voltage (2 to 12 kV) motor drives and are replacing electrolytic capacitors in lower voltage DC-link applications. This is due to a greater ripple current capability and life, lower equivalent series resistance and inductance, and "graceful" (non-catastrophic) failure of BOPP capacitors. The disadvantages of BOPP include a low dielectric constant of 2.2, which limits energy density, and maximum operating temperature of ca. 80 °C. Intensive research has been carried out on candidate material families for improved capacitive energy storage density, which include relaxor ferroelectric based copolymers [3], blends [4], nanolaminates [5], nanocomposites [6, 7] and modified glassy polymers through the incorporation of highly polar side groups such as cyanoethyl [8].

This paper highlights our rational co-design approach to the discovery and synthesis of new polymer dielectrics with largely improved capacitive energy storage density through the hierarchical search of a vast polymer chemical space based on first principles computation of dielectric constant and band gap, complemented with experimental validations through chemical synthesis and electrical characterization. Several classes of polymers including, but not limited to, polythioureas [9], polyimides [10, 11], polyureas and polyurethanes [12], polysulfones [13], and a new class of organotin polyesters [14-17] were targeted, synthesized, and characterized for dielectric properties. Select polymers and some of their properties are listed in Table 1.

Manuscript received on 12 September 2016, in final form 5 December 2016, accepted 6 December 2016. Corresponding author: Y. Cao.

DOI: 10.1109/TDEI.2017.006329

Table 1. Experimental dielectric constants, breakdown, and energy density for select new polymers along with BOPP, PET, and PPS as a benchmark comparison [18].

Polymer	Dielectric Constant	Operation Limit‡	Breakdown (MV/m)	Max Energy Density J/cm^3
BOPP	2.2	85°C	730	5
PET	3.3	125°C	570	4.7
PPS	3.0	200°C	550	4
PDTC-HK511	6.1	~80°C	602	9.8
BTDA-HK511	7.8	~75°C	676	15.8
BTDA-HDA	3.6	~150°C	812	10.4
Tin Polyester*	6.6	~250°C	500	7.3

‡Operation limit is taken as either onset of degradation for the tin polyester or onset of loss increase as the temperature approaches the glass transition. *Tin polyester is p[DMT(DMG-*co*-Sub)] with 80% content of DMG moiety.

2 ELECTRICAL CHARACTERIZATION

New polymers developed through this co-design effort were first vigorously characterized chemically to verify composition and purity and then characterized electrically as stated here. To analyze the dielectric properties, a series of electrical characterizations were conducted experimentally for dielectric constant, dielectric loss factor, DC breakdown strength, and charge-discharge hysteresis loop behavior.

2.1 TIME DOMAIN DIELECTRIC SPECTROSCOPY

Broadband dielectric spectroscopy was obtained through a combination of Time-Domain Dielectric Spectroscopy (TDDS) and frequency domain measurements (Novocontrol) over a wide frequency range of 0.01-1 MHz. A temperature range of +70 °C to -130 °C was used to study the local and segmental relaxations of the synthesized materials. Broadband Novocontrol was used to measure the dielectric loss spectra ε"(ω). Measurements were performed by placing the sample between two electrodes in parallel-plate capacitor geometry.

2.2 CHARGE-DISCHARGE HYSTERESIS LOOP

High-field polarization behavior under different voltage was characterized by a modified Sawyer-Tower polarization loop tester, employing a Trek Model 10/40 10 kV high voltage amplifier and an OPA541 operational amplifier-based current to voltage converter.

2.3 BREAKDOWN

Metalized films with aluminum metallization were used as the electrodes to ensure proper contact. A metal-insulator-metal (MIM) structure was formed with the top metalized film facing down and the bottom film facing up. A polyimide film with a 1.4 cm by 1.4 cm window in the center was used to control the contact active area. Before the measurement, the sample was conditioned to around 100 MV/m to generate sufficient electrostatic force in order to ensure good contact and elimination of any trapped air bubbles between the electrodes and the sample. The breakdown strength of the film samples was investigated using a linear voltage ramp of 300 V/s. When the first breakdown event occurred, the power supply was shut off through an interlock input by a silicon controlled rectifier (SCR) circuit, which uses the breakdown-induced ground-rise voltage capacitive coupled to the gate of an SCR. The breakdown voltage of the sample was read from a peak-holding voltmeter, and the data was analyzed using Weibull distribution.

3 COMPUTATIONAL GUIDANCE

Whereas materials discovery has traditionally centered around repeated experiments and testing, computational insights have helped steer it in a manner that is more rational than fortuitous. In the search for novel polymer dielectrics, it is known that significant portions of the polymer chemical universe remain unexplored, both because of the impracticality of synthesizing and testing hundreds of polymers and because of our inability to identify subspaces of promise. Thus, a reasonable starting point for our work was performing first-principles computations to study relevant properties of a selected subspace of organic polymers (such as shown in Figure 1) so as to obtain crucial guidance.

The organic polymers we considered for preliminary computations were formed by linear combinations of seven basic chemical building blocks shown in Figure 1a [19-22]. We performed density functional theory (DFT) [23] calculations as implemented in VASP [24] calculations on 267 such 4-block polymers; the computed dielectric constants are plotted against the computed band gaps in Figure 1b.

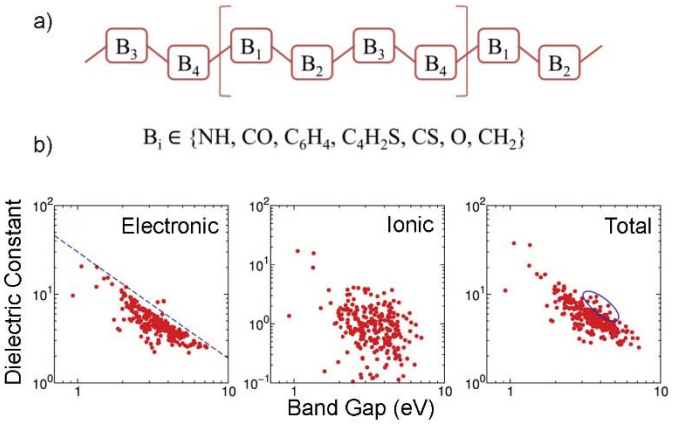

Figure 1. Organic polymers: DFT data. Reproduced with permission from [19]. Copyright (2016) John Wiley & Sons, Inc.

Though the electronic dielectric constant correlates inversely with the band gap and can thus only be increased so much without affecting the latter, the ionic dielectric constant has no such relationship. This results in a total dielectric constant and band gap plot as shown in Figure 1b, and the highlighted region contains promising candidates with respect to maximizing both properties. Three such candidates (belonging to distinct polymer subclasses: polyurea, polythiourea, and polyimide) were selected and synthesized, and their properties were measured [19, 20].

The main guidance emerging from this work was that a polymer should contain polar groups like NH or CO along with aromatic groups like C_6H_4 or C_4H_2S to achieve a relatively high dielectric constant with a sufficiently large band gap. Many newer polymers with arbitrarily long polymer

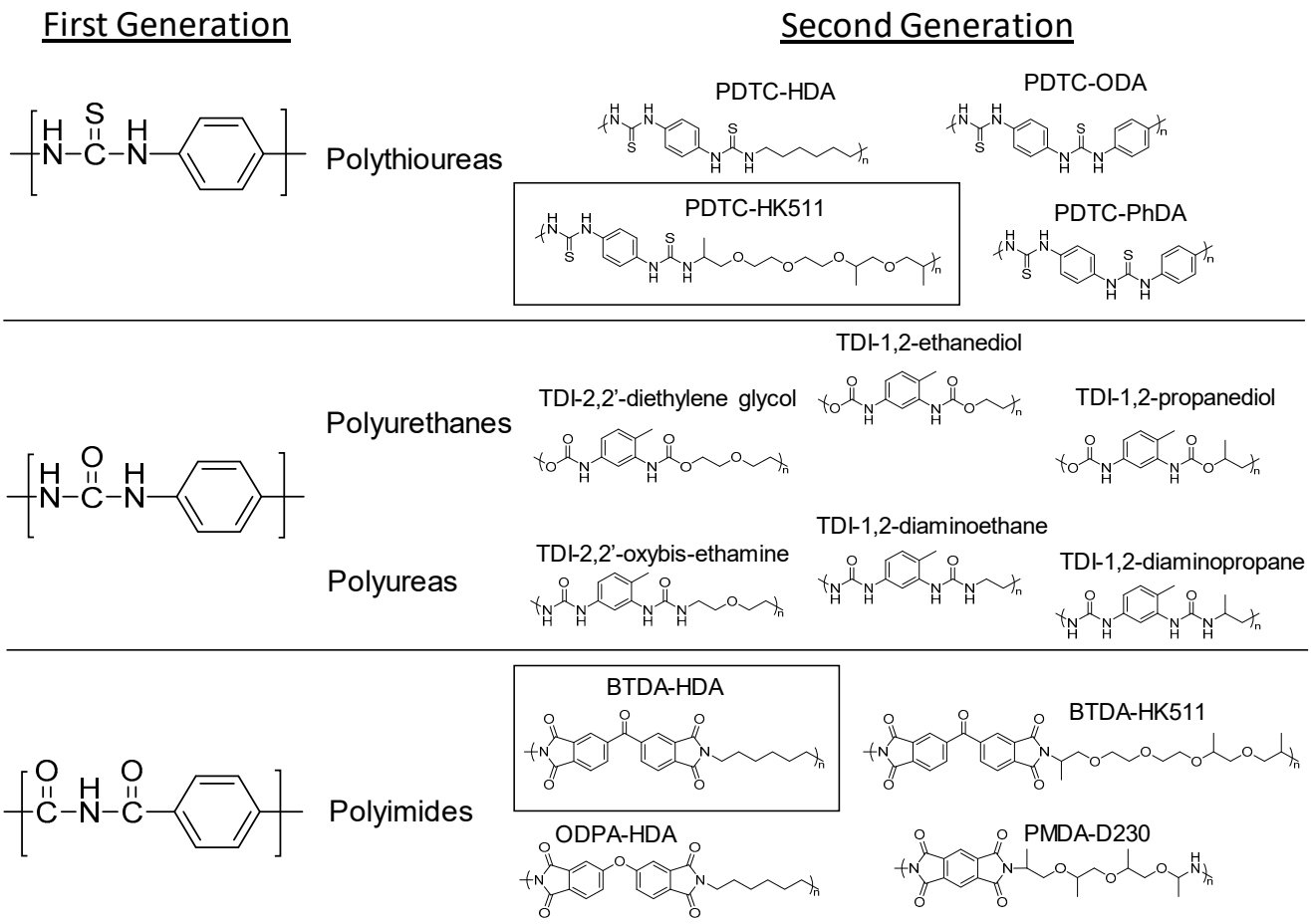

Figure 2. Synthetic scheme showing the transformation from the first generation of organic polymers to select polymers from the second generation. Reproduced with permission from [19]. Copyright (2016) John Wiley & Sons, Inc.

repeat units, which were not considered for computational purposes, were pursued. These contained desirable building blocks while providing easier synthetic routes, better processability, and attractive dielectric breakdown and loss behavior. The specific polymers thus designed are discussed in detail in Section 2 [9,10,13,16].

While the above computations led to many new and promising organic dielectric polymers, organometallic polymers were also studied based on the idea that introducing metal based units known to show high dielectric constants [21,25-27] in the polymer backbone would lead to improved properties. Figure 3 shows the predicted dielectric constants and band gaps of ca. 1000 polymers [28] that include the organic polymers from Figure 1, other new and well-known organic polymers, and different kinds of organometallic polymers based on nearly nine different metal atoms.

These computational results have formed the basis of the experimental realization of new, promising organometallic polymers and served to provide support and validation for experiments. A series of tin polyesters containing aliphatic, aromatic, and polar group linkers [14-17] have been designed and shown to display higher dielectric constants than their purely organic counterparts with similar band gaps.

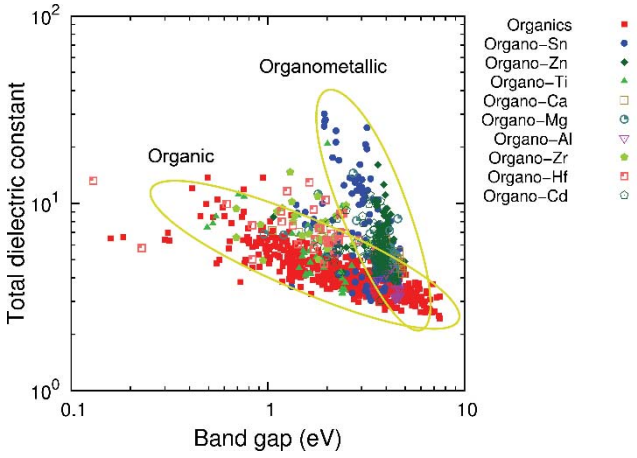

Figure 3. Comprehensive DFT generated database. Reproduced with permission from [19]. Copyright (2016) John Wiley & Sons, Inc.

While initial DFT computations helped understand the role of Sn atoms bonded to electronegative atoms in increasing the dielectric constant, further in-depth computations were performed on the Sn-polyesters to explore the dependence of their properties on the crystal structure and energetics. Similar calculations and experiments were conducted for Zn- and Cd-

polyesters; a detailed account of the various successes designing novel organometallic dielectric polymer candidates is given in Section 4.

Further, the computational data generated in the previously mentioned studies was used for performing machine learning, which helps unearth correlations between crucial polymer features as well as develop property prediction models. This involved a substantial 'fingerprinting' step, in which every polymer was converted to a unique representative vector based on its constituent building blocks. Following this, the fingerprint was mapped to the properties, leading to qualitative and quantitative insights that answer the following questions: (1) what kind of chemical blocks and combinations of blocks help increase the property being investigated and (2) how can the property be estimated solely as a function of the fingerprint?

This problem was solved for the smaller dataset of organic polymers in Figure 1 [22]. Specific blocks and block pairs were identified that increase or decrease the dielectric constant or band gap (for instance, CH_2-CH_2 and CH_2-O pairs increase the band gap but decrease the electronic dielectric constant), and models were trained using Kernel Ridge Regression [22,29] to predict the dielectric constant and band gap of any new n-block polymer simply by converting it to its fingerprint. As a result, quick predictions were able to be made for thousands of new polymers with arbitrary repeat units, thus further populating the plots in Figure 1 and providing increased guidance to experiments. Machine learning techniques are currently being used on the entire dataset shown in Figure 3 in order to enhance insights into a much wider chemical space.

4 FROM COMPUTATIONS TO SYNTHESIS

Initial theoretical predictions were provided to the synthetic group to determine synthetically viable polymers. Three classes of organic polymers (polythioureas, polyimides, and polyureas/urethanes) and a class of organometallic polymers containing tin were selected for initial synthesis. In all four cases, three generations or cycles of this rational co-design process were followed, and experimental results were transferred back to the computational group to guide further experimentation and optimization. To give an understanding of the sheer size of potential polymers here, the original 267 polymers that were predicted using a 4-block approach were later expanded to over 150,000 polymers for multiple block organic systems. Before synthesis could take place, a large effort was required to rationally narrow this field and subsequently decide which polymers to include in order to increase the scope of the study. Figure 2 shows the three first generation polymers next to a small sample of their respective second generation classes that were synthesized. Showing the large amount of materials made during this synthetic effort would be unwieldy and impractical. The following sections briefly outline this co-design approach and a couple of the more promising polymers are highlighted in further detail.

4.1 FIRST GENERATION ORGANIC POLYMERS

The first generation of organic polymers is reported in detail in [20], which outlines the first iteration of this rational design process before there was much co-design involved. Three polymers were synthesized with each containing the characteristic chemical linkages of a thiourea group, a urea group, and an imide group, as shown on the left side of Figure 2. To ensure these polymers could be matched with the first round of computational predictions, the repeat unit was constrained to the same four chemical blocks that were used in synthesis as for simulation. Unfortunately, this caused these first generation polymers to be insoluble in nearly all solvents and non-melt processable due to their high intermolecular attractions. However, the electronic properties of these polymers, such as dielectric constant and band gap, were shown to have close agreement between real and predicted results. Furthermore, the structural morphologies predicted from computations were validated through experimental X-Ray diffraction. From these initial successes, data was transferred back to the computational team to help guide the next generation of polymers to be synthesized. As stated in Section 3, it was shown that including sulfur, oxygen, and nitrogen was beneficial in improving dielectric constant. The synthetic chemists were able to expand the size of the repeat unit in an effort to break up intermolecular interactions and produce soluble and processable polymers.

4.2 SECOND GENERATION ORGANIC POLYMERS

After the initial success of matching targeted polymers to their predicted properties, more guidance was needed to design the second generation of polymer synthesis experiments. For the first generation, the 4-block limitation only gave ca. 300 choices of polymers with only one-hundredth of them actually being synthesized; however, once the chain expanded to include four, six, and eight blocks, the number of possible polymers increased drastically to upwards of 150,000 unique polymers. Typically, this would be seen as an impossible task following the traditional Edisonian approach of trial and error; instead, guidance from computations and the engineers testing the polymers enabled the field of potential polymers to be down selected to around ten polymers for each class. It was then feasible to synthesize and characterize these 30 organic polymers while in-depth calculations were being run by the computational team. These secondary computations required much longer computation times and processing power compared to the initial screening. Just like synthesis in the laboratory, they had to be carefully chosen as to not waste valuable computational resources. Rapid feasibility studies of polymers from such a vast pool of potential candidates would not be possible without this co-design approach. For the sake of brevity and to avoid getting too deep into experimental details that may not be of interest to the IEEE audience, the following discussion briefly covers polythioureas while highlighting work done on two promising polythioureas and a single polyimide.

4.3 EXPANSION INTO POLYTHIOUREAS

From the initial work on first generation polymers, it was apparent that sulfur was instrumental in improving the dielectric constant of polymers due to its relatively large and polarizable electron cloud. The simplest and most stable way found to incorporate sulfur directly into the polymer chain was through the polythiourea. These polymers replace the oxygen found in traditional polyureas with a sulfur atom and have recently received heightened attention for dielectric applications [30-33]. Several polymers were synthesized using the same basic starting molecule, para-phenylene diisothiocyanate (PDTC), and reacting it with numerous diamines as seen in [34] with their properties shown in Table 2. This method was shown to produce high molecular weight polymers, which subsequently were able to be solution cast and produced thin films for characterization. The selection of diamines was driven by a desire to gain further understanding of the properties imparted by different chemical groups. Another important consideration for this project was the reduction of the cost of the final polymer as much as possible through the use of commercially available monomers instead of specialty made monomers, which would be unrealistic to produce on a commercial scale. This was accomplished by choosing three very similar diamines to see the effect of a single benzene ring: two benzene rings attached through a carbon and a replacement of that carbon linker with an oxygen atom. In addition, a diamine with only hydrocarbons was chosen as a less polar control along with an industrially produced ether-containing diamine from Huntsman called Jeffamine HK511.

Table 2. Experimental dielectric constant (ε), Tan δ and band gap (E_g) for second generation polythioureas with predicted values from DFT or machine learning in parenthesis [9].

Polythiourea	ε (r.t. 1kHz)	Tan δ (r.t. 1kHz)	E_g (eV)
PDTC-ODA	4.52 (5.42)	0.0233	3.22 (3.45)
PDTC-MDA	4.08 (4.59)	0.0348	3.16 (3.25)
PDTC-PhDA	4.89 (5.55)	0.0144	3.07 (2.54)
PDTC-HDA	3.67 (4.01)	0.0267	3.53 (3.68)
PDTC-HK511	6.09 (5.76)	0.0115	3.51 (4.79)
Thiophosgene-MDA	3.84 (4.58)	0.0226	3.30 (3.28)

As theorized, the dielectric constant of the polythiourea made with an oxygen linking the benzene rings (PDTC-ODA) was found to be higher than that of the polymer with a carbon linker (PDTC-MDA) (4.5 vs. 4.1). The polymer made with the hydrocarbon diamine (PDTC-HDA) was shown to have the lowest dielectric constant (3.7) as expected since the chain lacked any additional polarity over the base thiourea group. Finally, the polythiourea made from Jeffamine HK511 (PDTC-HK511) had the highest dielectric constant (6.1) due to the enhanced polarizability of the ether-containing diamine segment as well as a slight increase in free volume from side groups to allow the chains to give orientational polarization. The one drawback of using HK511 is that the flexible ether chain reduces the glass transition temperature (T_g) from 139 °C for the aliphatic linker to 92 °C for PDTC-HK511.

A separate polythiourea was also synthesized for this study using thiophosgene in place of PDTC. This was to show that polymers similar to the ones shown here could be produced in higher molecular weights through this industrial scale reaction. This polymer, Thiophosgene-MDA, was also previously synthesized by Zhang [32] through the use of a microwave polymerization and was shown to have desirable properties. One drawback of microwave polymerization was that it produced a much lower molecular weight on the order of 4,000 g/mol compared to that of 44,600 g/mol by thiophosgene. Through the use of thiophosgene and commercially available diamines, high molecular weight polythioureas with improved film-forming qualities and a relatively low cost could be synthesized with high dielectric constants and correspondingly high energy densities.

4.4 INVESTIGATION OF PROMISING EXAMPLES

Two notable polythioureas, PDTC-HK511 and Thiophosgene-MDA, were chosen to showcase further characterization and results. First, 30 separate breakdown measurements were taken on thin films for each of the polymers, and the results were subjected to Weibull analysis as described in Section 2. Figure 4 shows the Weibull distribution of breakdown strength with breakdown strength being greater than 600 MV/m for each polymer. The electrical testing on dielectric constant and breakdown suggest an upper limit of energy density of 9.8 J/cm^3 for PDTC-HK511 and 7.8 J/cm^3 for Thiophosgene-MDA, nearly double BOPP's maximum energy density of 5 J/cm^3.

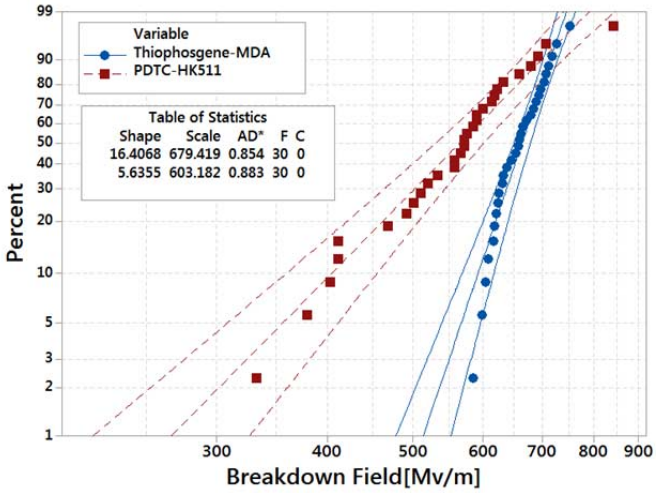

Figure 4. Breakdown field for polythioureas, Thiophosgene-MDA, and PDTC-HK511.

High-field polarization behavior was characterized as shown in Figure 5 with both polymers displaying linear polarization behavior. The D-E loop for Thiophosgene-MDA is shown in Figure 5a and indicates a breakdown strength approaching 700 MV/m. The D-E loop for PDTC-HK511 in Figure 5b achieved a breakdown strength of 550 MV/m before failure in close agreement with the multi-sample Weibull analysis. From the slope of the D-E loop, the dielectric constant was calculated to be ca. 6, which agrees very well with the low field broadband dielectric spectrum data. The total

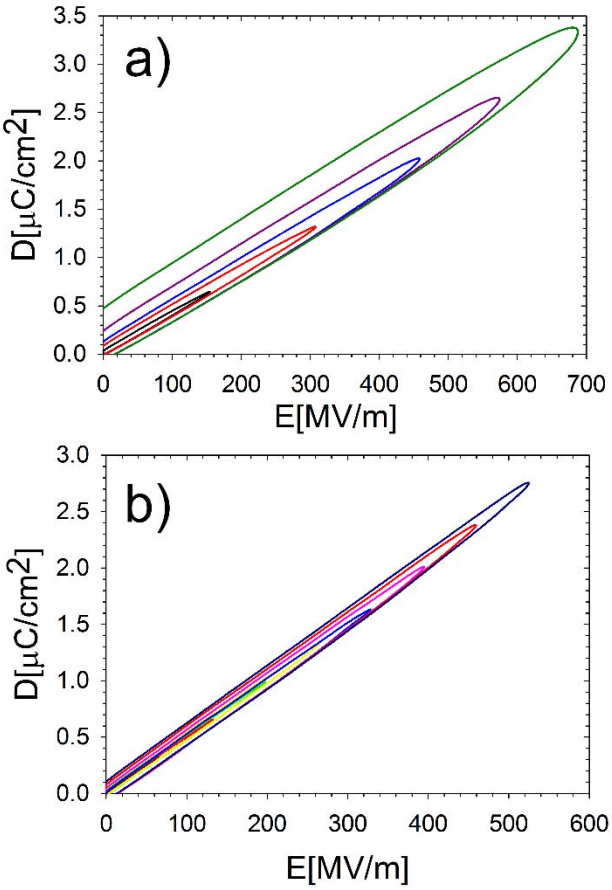

Figure 5. D-E loop of polythioureas (a) Thiophosgene-MDA, (b) PDTC-HK511.

loss is calculated by the area enclosed by the D-E loop. That loss combines the dipolar loss with conduction loss that is observed at the high electric fields. High-field conduction losses can be associated with small molecules within the polymer films such as residual solvents and reaction by-products that were not entirely removed during synthesis and processing. In addition, other processing issues such as outside contaminants or dust can interfere with the film quality, and laboratory scale processing can leave the films to not be 100% defect free. As the reaction conditions are optimized and thin film processing improved, there is an expectation and some initial evidence that this conduction loss could be significantly decreased. The released energy is calculated by integrating the D/E curve. High discharge efficiency is obtained by computing the ratio of released energy to the total stored energy density as shown in Figure 6. The discharge efficiency will improve in a similar manner with the reduction of conduction loss.

To further explore the relation between a material's molecular architecture and its electrical properties, a study on the relaxation mechanisms was required. Here, PDTC-HK511 was measured on a Novocontrol instrument from 0.01 Hz - 1 MHz and a temperature range from -130 °C to 70 °C to analyze any sub glass transition temperature phenomenon [35]. 3D plots of the Novocontrol results are shown in Figure 7a and Figure 7b displaying the real and the imaginary parts,

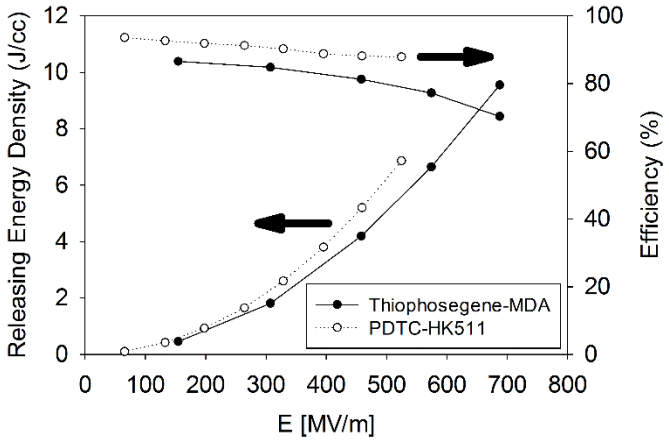

Figure 6. Releasing energy densities vs. applied electric field of polythioureas Thiophosgene-MDA, and PDTC-HK511

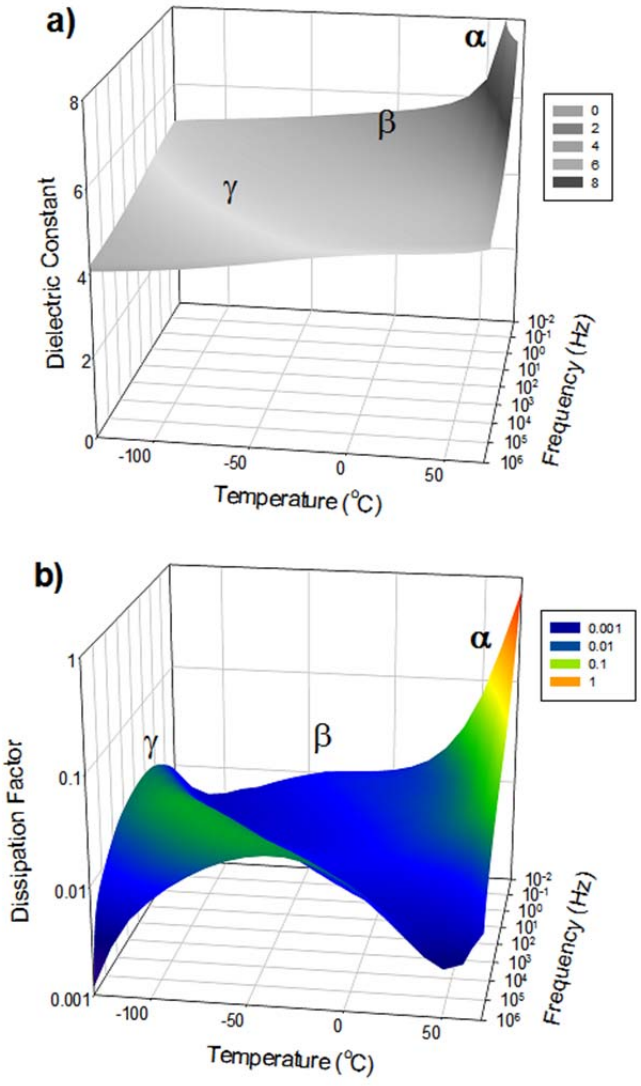

Figure 7. The 3D plots of the real (a) and imaginary (b) parts of the complex dielectric spectroscopy for thiourea–etheramine copolymer over a frequency range of 0.01Hz-1MHz and a temperature range from -130 °C to +70 °C. Reproduced with permission from [35]. Copyright (2015) IEEE.

respectively, resulting in dielectric constant and dissipation versus frequency and temperature spectra. A peak recorded at 70 °C shows the onset of additional chain mobility, which begins around the glass transition of the polymer and is designated the α peak. Before this peak occurs, the dielectric constant is between 5.5 and 6, similar to what was determined through TDDS and D-E loop measurements. As the temperature drops, a depression valley is shown where the dielectric constant drops to ca. 5 and loss drops below 1% for certain frequencies and is labeled as the β peak. As the temperature is reduced further, another relaxation peak is shown and set as the γ peak with the dielectric constant approaching ca. 4 and loss increasing to ca. 10%. With a further reduction in temperature to -130 °C, the dielectric constant rests at 4 and the loss drops off to 0.01% for some frequencies. It is predicted that these transitions below the glass transition temperature are localized secondary relaxations due to rotational movements in chain dipoles [36]. In the case of PDTC-HK511, these movements could be explained by the flexible ether chain with sidechain methyl groups giving the dipoles the free volume they need to rotate freely. A model for secondary glass transitions peaks has been postulated in the Havriliak-Negami (HN) function [37]

$$\epsilon(\omega) - \varepsilon_\infty = \frac{\Delta\varepsilon}{[1+(i\omega\tau)^\alpha]^\beta} \quad (1)$$

where ω=2π*f*, Δε is the relaxation strength, while α and β are the shape factors for the width and symmetry of the loss peak, respectively. These are independent from the unrelaxed optical permittivity ε_∞ and the relaxation time τ described through an Arrhenius styled equation.

$$f_{max} = f_{max,\infty} e^{\left(-\frac{E_a}{k_B T}\right)} \quad (2)$$

Isothermal plots were generated from the Novocontrol data to further investigate each relaxation. The β and γ relaxations are shown in Figure 8a and 8b, respectively. To characterize the shape factors and the dielectric intensity of a loss peak, a more detailed analysis based on HN model function was required. However, a first order of accuracy relaxation mapping allows the activation energies to be derived with β and γ having energies of 0.45 eV and 0.14 eV, respectively, and plotted in Figure 8c. The low activation energy of these secondary relaxations indicated that the ether dipoles are able to participate and be oriented in the presence of an electric field and contribute to the orientational polarization in the dielectric constant. The "frozen" dielectric constant at -130 °C is ca. 4, similar to previously synthesized aromatic polythioureas that lacked the flexible ethers and whose dielectric constant more closely resembled the predicted electronic and ionic portions of the dielectric constant from first principles calculations [9], [33].

4.5 HIGHER TEMPERATURE POLYIMIDES

Polyimides have been known to be effective dielectrics with stability across a large temperature range as seen in the well-known material Kapton developed by DuPont. Therefore, it came as no surprise that a polyimide type material would be identified by computational predictions for a dielectric material. Due to the solubility issue of the first generation of polyimide synthesized with a 4-block design, a similar expansion was performed on polyimides as was done for polythioureas.

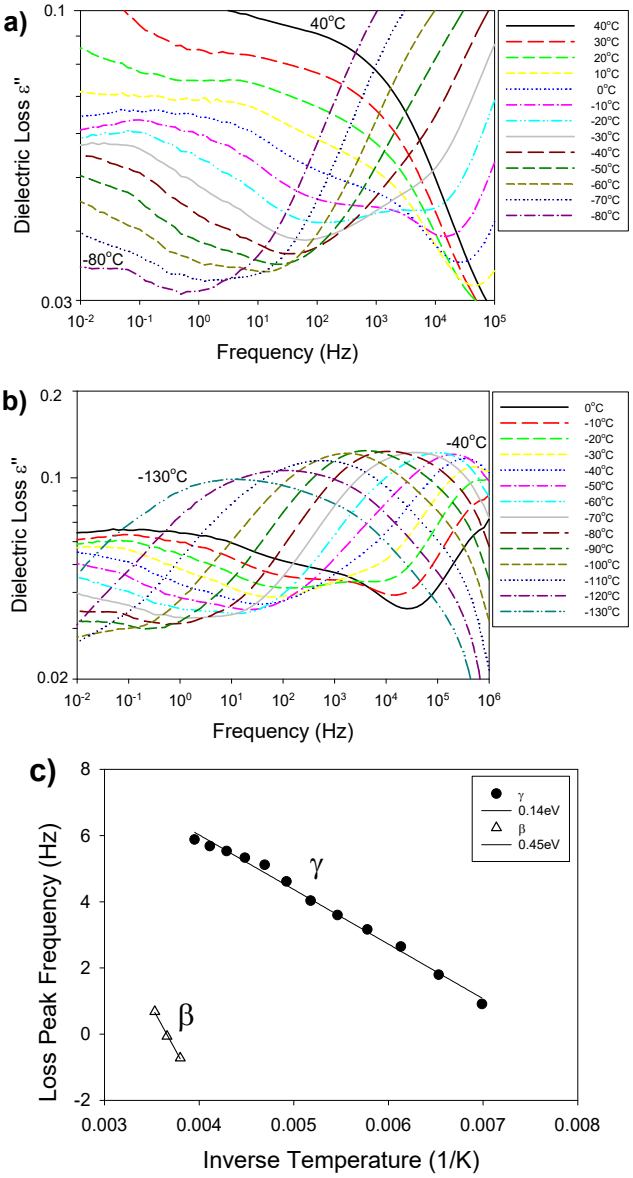

Figure 8. The isothermal plots of the dielectric spectrum data showing the β transition (a) and γ transition (b), as well as the corresponding relaxation map (c) for both β and γ transitions as according to Arrhenius equation. Compared with the α relaxation peak, these secondary relaxation peaks are much broader and often nonsymmetrical. Reproduced with permission from [24]. Copyright (2015) IEEE.

There were two variables that could be changed during synthesis of polyimides. The first variable was the dianhydride unit, of which five were chosen in a similarly rational way to the polythiourea selection. Aromatic dianhydrides were chosen with different bridges or linkers between the aromatic groups such as a carbon, an ether, a carbonyl, and a fluorinated carbon linker. In addition, pyromellitic

didianhydride (PMDA), which is the same dianhydride used in Kapton synthesis, with no linker was chosen. The second variable that could be adjusted was the diamine, which was adjusted with the polythiourea study. In this case, two separate aliphatic diamines were used: one with 3 CH_2 spacers and the other with 6 CH_2 spacers. Jeffamine HK511 was again used as a diamine as well as Jeffamine D230, which has a more regular chain than HK511 but is also an etheramine produced by Huntsman. By using these four diamines, the effect of both the dianhydride and diamine units could be studied in tandem, and select results are shown in Figure 9.

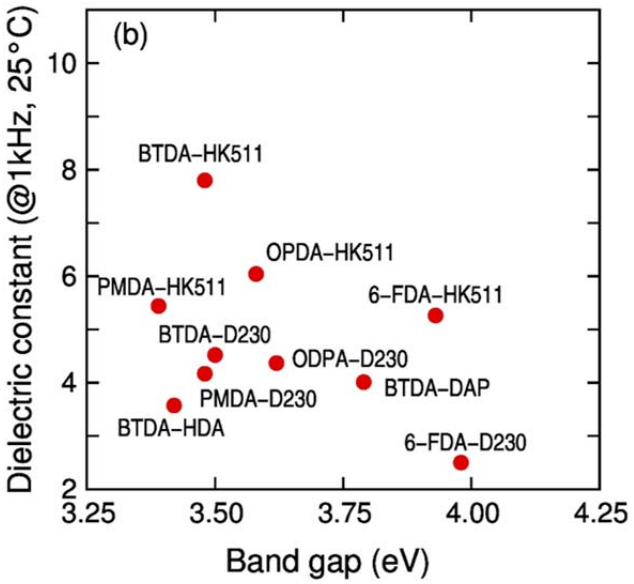

Figure 9. Dielectric constant and band gaps of select second generation polyimides. Reproduced with permission from [19]. Copyright (2016) John Wiley & Sons, Inc.

Overall, it was found that combining the dianhydride with a carbonyl linker, 3,3′,4,4′-benzophenone tetracarboxylic dianhydride (BTDA), and HK511 had the highest dielectric constant of 7.8 at a frequency of 1 kHz and in a 25 °C environment but suffers from a lower glass transition ca. 78 °C. However, the polymer with a 6 CH_2 unit spacer produced from the carbonyl containing dianhydride, BTDA-HDA, was found to have the best film forming qualities. Despite a modest dielectric constant of 3.6 and loss below 1%, BTDA-HDA showed good thermal stability with a glass transition temperature of 150 °C and the ability to be melt processable with a melt transition ca. 230 °C. Figure 10 shows 25 independent breakdown tests conducted on BTDA-HDA with a Weibull analysis resulting in a breakdown field ca. 800 MV/m, which corresponds to a maximum energy density of ca. 10 J/cm^3. The polyimides BTDA-HDA and BTDA-HK511 showed maximum theoretical energy densities of 9.98 J/cm^3 and 15.77 J/cm^3, which are double and triple that of BOPP, respectively. This is a significant improvement over the first generation of polyimides, which were insoluble and had improved to not just be soluble but also melt processable, enabling various processing and post-processing improvements to be carried out on the material such as stretching or annealing. As a result, further studies have been conducted on this polyimide in an attempt to improve the dielectric constant while maintaining a high breakdown and energy density. It has previously been hypothesized that for a polar polymer, enhancement in the dielectric constant is due to the amorphous regions of the film and any semi-crystalline regions decrease the dielectric constant [38]. By increasing the amount of amorphous region in the polymer film through these processing techniques, the dielectric constant has been shown to increase [39, 40].

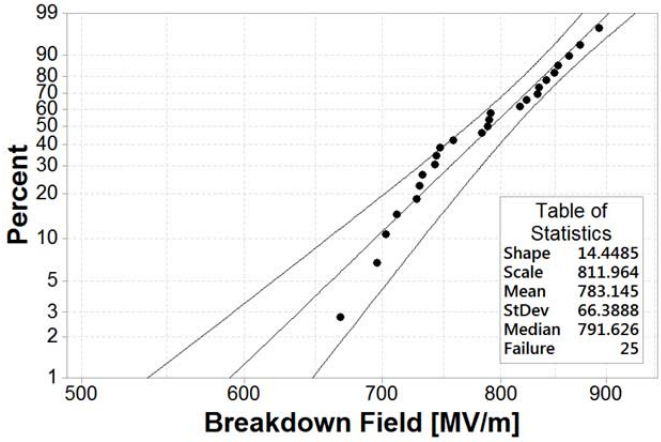

Figure 10. Weibull distribution for the polyimide BTDA-HDA. Reproduced with permission from [10]. Copyright (2014) American Chemical Society.

5 ORGANOMETALLIC POLYMERS

After extensive computational work, first principles DFT predictions found a benefit for the incorporation of more electropositive metal atoms into the polymer backbone by means of covalent bonds [15]. The predictions show an enhancement of the dipolar and atomic polarization due to the low electronegativity of metals with large electron clouds and low-frequency lattice vibrations improved the dielectric constant [19]. Additionally, the incorporation of the metal directly into the chain should alleviate any dispersion issues that normally accompany nanocomposites [41]. Organometallic polymers, which have highly electropositive metal atoms covalently bonded to the backbone, occupy a different subspace than the organic polymers and are considered for the next generation of energy storage materials due to the large electronegativity difference between metal and oxygen [19]. As stated previously, tin containing organometallic polymers were desirable for initial synthesis due to their impressive electrical properties found in DFT computations. Their ionic dielectric constants (ε_{ion}) are higher than that of other members of group 14 elements such as Si, Ge, and Pb, which contributed to a high total dielectric constant.

5.1 INITIAL ORGANOTIN SYNTHESIS

Initially, dimethyltin (DMT) dichloride was considered with various diacids to synthesize tin polyesters, p[DMT$(CH_2)_n$], allowing for a larger dipolar and atomic polarization within the polymer chain. The repeat unit with dimethyl tin bonded to

oxygen is shown in Figure 11 where R represents an aliphatic chain of length n.

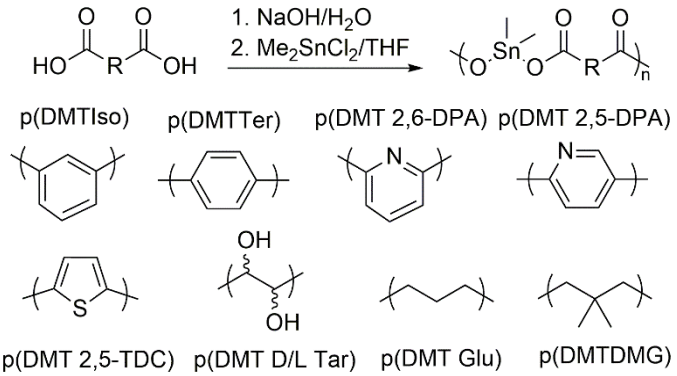

Figure 11. The general synthetic route for the preparation of poly(dimethyltin esters) along with select monomers Reproduced with permission from [19]. Copyright (2016) John Wiley & Sons, Inc.

Many low energy structures of the same motif were predicted for each polymer system. The general trend showed that the dielectric constant increased and bandgap decreased when n was decreased, as shown in Figures 12a and 12b [15]. Among this family of diacid systems, poly(dimethyitin glutarate) (pDMTGlu) and poly(dimethyltin suberate) (pDMTSub) with three and six methylene spacers, respectively, showed promise due to their higher dielectric constant ca. 6-7 and better thermal stability compared to BOPP.

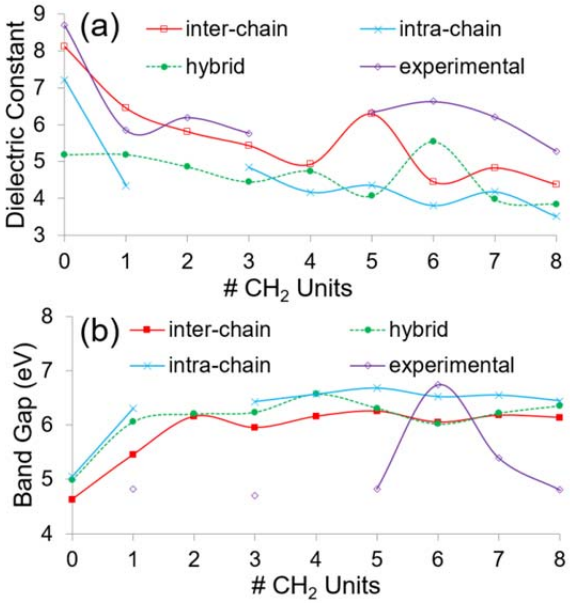

Figure 12. Computed and measured data for a) dielectric constants and b) bandgaps of the poly(dimethyltin esters) in different motifs (α, β, and γ) with various linker lengths, ranging from 0 to 11 methylene (CH2) units. Reproduced with permission from [15]. Copyright (2015) American Chemical Society.

The blend consisting of 20% p(DMTDMG) with 80% p(DMTSub) by weight showed a breakdown strength of ca. 300 MV/m and ener3gy density of ca. 4 J/cm^3, as shown in the D-E hysteresis loop in Figure 10c [41].

5.2 EXPANSION OF ORGANOTIN POLYESTERS

Other systems such as aromatic rings and chiral or asymmetric groups were introduced as building blocks in the organometallic polymers to investigate the effect on electrical properties [16]. These systems can be divided into three categories: electron-withdrawing pyridine, electron-donating thiophene, and electron "neutral" benzene rings. Poly(dimethyltin isophthalate) (p(DMTIso)), poly(dimethyltin 2,6-dipicolinate) (p(DMT 2,6-DPA)), and poly(dimethyltin 2,5-thiophenedicarboxylate) (p(DMT 2,5- TDC) exhibit higher average dielectric constants of 5.5, 5.6, and 5.1, respectively[16], while the diacids used in these polymers were in the meta position. On the contrary, poly(dimethyltin terephthalate) (p(DMTTer)) and poly(dimethyltin 2,5-dipicolinate) (p(DMT 2,5-DPA)) have dielectric constants of 4.7 and 4.8, respectively, where the diacids are present in ortho and para position [16]. The sulfur-containing aromatic ring, thiophene, is electron rich, whereas pyridine is electron deficient due to the localization of ring current around nitrogen, which results in an uneven electron density in the ring. On the contrary, benzene is electron neutral as it has an evenly distributed ring current. The incorporation of aromatic rings was shown to favorably improve the thermal stability to ca. 250 °C. The dielectric loss of these polymers was < 3% with the lowest loss polymer, p(DMTIso), was found to be as low as 0.39% [16]. The higher dielectric losses can be attributed to the presence of residual water. However, as previously mentioned, crystallinity in the polymer backbone can have a negative effect on the dielectric constant, leading to a desire for amorphous polymers [33]. This can be achieved by employing a diacid that contains chiral or asymmetric centers. Chiral tartaric acid with its D- and L- forms can increase the amorphous region in the polymer chain by disrupting the chain packing through steric hindrance in the -OH group. For comparison, more crystalline polymers were synthesized using DL-tartaric acid, a mixture of both forms. The amorphous and crystalline nature of the polymers was confirmed by X-Ray diffraction patterns. These polymers showed higher dielectric constants ca. 5.3 and 5.5 for D- and L-tartaric acid polymers, respectively, with a dielectric constant of 5.0 for the racemic DL-tartaric acid polymers. These results show that a higher dielectric constant correlates with less crystallinity [16].

5.3 OPTIMIZATION OF ORGANOTIN POLYESTERS

The previously made organotin polyesters have a tendency to form large crystalline phases after drop casting and drying due to the regularly repeated and polar nature of their chain segments. For a third-generation study, an optimization of aliphatic tin polyester systems was carried out not only to improve morphological properties but also to enhance electrical properties. Poly(dimethyltin suberate), p(DMTSub), was chosen as it had the highest reported dielectric constant as measured from a pressed powder pellet [17]. To disrupt the chain packing to give a more amorphous film morphology, p(DMTSub) was blended with a new homopolymer, poly(dimethyltin 3,3,-dimethylglutarate), p(DMTDMG),

which has two CH_3 groups sticking out from the center of the chain to interrupt close packing of chains. Blends and copolymers of p(DMTSub) with p(DMTDMG) were prepared with varying mass ratios from 10% to 50% wt/wt of p(DMTSub). The crystalline nature of p(DMTSub) is shown in Figure 13a, while the effect of p(DMTDMG) on producing amorphous blends and copolymers is shown in Figure 13b. Among five blend systems and five copolymer systems, the blends and copolymers with 90% DMG moiety showed the highest dielectric constants of almost 7, which surpassed the values of both homopolymers. Due to their blended and copolymerized nature, all resulting polymers had a band gap ca. 4.8 eV, similar to p(DMTDMG), which should lead to a high breakdown field. Interestingly, the blend with 20% p(DMTSub), BP20, and copolymer with 20% p(DMTSub), CP20, both exhibited the same high dielectric constant of 6.6.

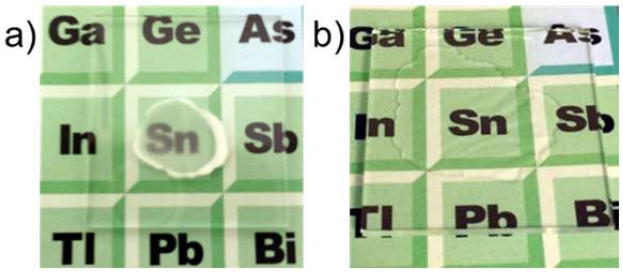

Figure 13. Tin ester films cast on glass microscope slides to show the crystallinity in (a) p(DMTSub) and (b) an amorphous blend of 30% p(DMTSub) and 70% p(DMTDMG). Reproduced with permission from [17]. Copyright (2016) American Chemical Society.

The first D−E hysteresis loops for the tin polyester system were carried out on BP20 and CP20 due to parity in their dielectric constants. The blend BP20 was seen to withstand a field of ca. 300 MV/m before breakdown with an energy density of ca. 4 J/cm^3 [15]. The copolymer CP20 was seen to withstand an enhanced field ca. 500 MV/m before breakdown with a maximum energy density ca. 6 J/cm^3 and 85% efficiency at the breakdown as shown below in Figure 14 [17].

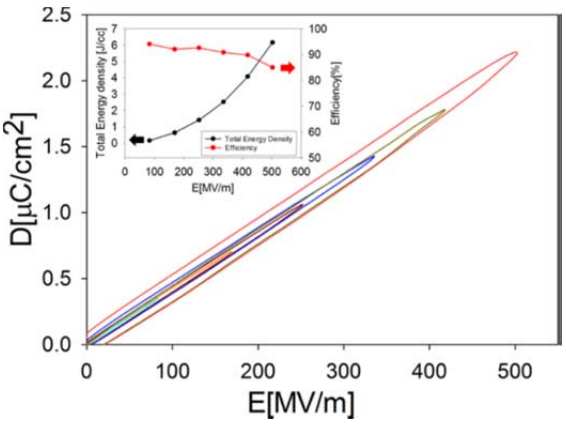

Figure 14. D−E hysteresis loop for CP20 along with an inset showing the corresponding total energy density and efficiency plot. Reproduced with permission from [17]. Copyright (2016) American Chemical Society.

6 CONCLUSIONS

This article has attempted to convince the reader of the practicalities of coupling together computations, synthesis, and characterization to aid in the discovery and optimization of new materials. We have outlined an approach starting from first principles calculations and later machine learning techniques to develop a dataset of polymers with predicted properties. The favorable polymers were targeted for initial synthesis and characterization as a first generation, followed by two successive iterations. At the end of the third generation, several polymers were identified with high dielectric constants, low loss, high thermal stability, and improved energy densities over BOPP and are shown in Table 1 alongside several common film dielectric polymers for comparison. Through the continuation of this rational co-design loop, new polymers with targeted properties can be rapidly synthesized and characterized to screen for desirable properties and speed up the development of next-generation materials. While rational co-design through hierarchical searches of chemical space continues, fundamental understanding of the degradation and breakdown of new polymer dielectrics should be advanced. This is in large part because engineering breakdown field and dielectric loss, two key parameters for film capacitors, cannot yet be predicted from first principles since dielectric relaxation, high-field degradation, and breakdown at engineering fields are extremely complex phenomena. Concerted co-design and development will continue towards the ultimate goal of developing high energy density polymer dielectrics.

ACKNOWLEDGMENT

This work is supported through a multidisciplinary university research initiative (MURI) grant through the Office of Naval Research (N00014-10-1-0944). The authors would like to acknowledge Dr. Steven Boggs and Dr. Miko Cakmak for their valuable insight and JoAnne Ronzello for performing TDDS measurements.

REFERENCES

[1] T. Heidel, "Grid power flow control and optimization," Carnegie Mellon Electricity Industry Center Seminar, Pittsburgh PA, 2013.

[2] "Department of Energy Vehicle Technologies Office 2015 Energy Storage R&D Annual Report," Washington DC, USA, 2015.

[3] B. Chu, X. Zhou, K. Ren, B. Neese, M. Lin, Q. Wang, F. Bauer and Q. M. Zhang, "A dielectric polymer with high electric energy density and fast discharge speed," *Science.*, Vol. 313, No. 5785, pp. 334–336, 2006.

[4] S. Wu, M. Lin, S. G. Lu, L. Zhu, and Q. M. Zhang, "Polar-fluoropolymer blends with tailored nanostructures for high energy density low loss capacitor applications," Appl. Phys. Lett., Vol. 99, No. 13, pp. 7–10, 2011.

[5] M. Mackey, D. E. Schuele, L. Zhu, L. Flandin, M. A. Wolak, J. S. Shirk, A. Hiltner, and E. Baer, "Reduction of dielectric hysteresis in multilayered films via nanoconfinement," Macromolecules, Vol. 45, No. 4, pp. 1954–1962, 2012.

[6] K. Yang, X. Huang, J. He, and P. Jiang, "Strawberry-like core-shell Ag@polydopamine@BaTiO 3 hybrid nanoparticles for high- k polymer nanocomposites with high energy density and low dielectric loss," Adv. Mater. Interfaces, Vol. 2, pp.1500361-1500371, 2015.

[7] X. Huang and P. Jiang, "Core-shell structured high- k polymer nanocomposites for energy storage and dielectric applications," Adv. Mater., Vol. 27, No. 3, pp. 546–554, 2015.

[8] J. T. Bendler and T.Takekoshi, "Molecular modeling of polymers for high energy storage capacitor applications," IEEE 35th Int'l. Power Sources Sympos., Cherry Hill, NJ, USA, pp. 373-376, 1992.
[9] R. Ma, V. Sharma, A. F. Baldwin, M. Tefferi, I. Offenbach, M. Cakmak, Y. Cao, R. Ramprasad, and G. A. Sotzing, "Rational design and synthesis of polythioureas as capacitor dielectrics," J. Mater. Chem. A, Vol. 3, pp. 14845–14852, 2015.
[10] R. Ma, A. F. Baldwin, C. Wang, I. Offenbach, M. Cakmak, R. Ramprasad, and G. A. Sotzing, "Rationally designed polyimides for high-energy density capacitor applications.," ACS Appl. Mater. Interfaces, Vol. 6, No. 13, pp. 10445–51, 2014.
[11] A. F. Baldwin, R. Ma, C. Wang, R. Ramprasad, and G. a. Sotzing, "Structure-property relationship of polyimides based on pyromellitic dianhydride and short-chain aliphatic diamines for dielectric material applications," J. Appl. Polym. Sci., Vol. 130, No. 2, pp. 1276–1280, 2013.
[12] R. G. Lorenzini, W. M. Kline, C. C. Wang, R. Ramprasad, and G. A. Sotzing, "The rational design of polyurea & polyurethane dielectric materials," Polymer, pp. 1–5, 2013.
[13] R. G. Lorenzini, J. A. Greco, R. R. Birge, and G. A. Sotzing, "Diels–Alder polysulfones as dielectric materials: Computational guidance & synthesis," Polymer, Vol. 55, No. 16, pp. 3573–3578, 2014.
[14] A. F. Baldwin, R. Ma, A. Mannodi-Kanakkithodi, T. D. Huan, C. Wang, M. Tefferi, J. E. Marszalek, M. Cakmak, Y. Cao, R. Ramprasad, and G. a Sotzing, "Poly(dimethyltin glutarate) as a prospective material for high dielectric applications.," Adv. Mater., Vol. 27, pp. 346–351, 2014.
[15] A. F. Baldwin, T. D. Huan, R. Ma, A. Mannodi-Kanakkithodi, M. Tefferi, N. Katz, Y. Cao, R. Ramprasad, and G. A. Sotzing, "Rational Design of Organotin Polyesters," Macromolecules, Vol. 48, No. 8, pp. 2422–2428, 2015.
[16] A. F. Baldwin, R. Ma, T. D. Huan, Y. Cao, R. Ramprasad, and G. A. Sotzing, "Effect of Incorporating Aromatic and Chiral Groups on the Dielectric Properties of Poly (dimethyltin esters)," Macromol. Rapid Commun., Vol. 35, No. 24, pp. 2082–2088, 2014.
[17] G. M. Treich, S. Nasreen, A. M. Kanakkithodi, R. Ma, M. Te, J. Flynn, Y. Cao, R. Ramprasad, and G. A. Sotzing, "Optimization of organotin polymers for dielectric applications," ACS Appl. Mater. Interfaces, Vol. 8, No. 33 pp. 21270-21277, 2016.
[18] M. Rabuffi, G. Picci, "Status quo and future prospects for metallized polypropylene energy storage capacitors," IEEE Trans. Plasma Sci., Vol. 30, No. 5, pp. 1939–1942, 2002.
[19] A. Mannodi-Kanakkithodi, G. M. Treich, T. D. Huan, R. Ma, M. Tefferi, Y. Cao, G. A. Sotzing, and R. Ramprasad, "Rational co-design of polymer dielectrics for energy storage.," Adv. Mater. Prog. Rep., Vol. 28, No. 30 pp. 6277-6291, 2016.
[20] V. Sharma, C. Wang, R. G. Lorenzini, R. Ma, Q. Zhu, D. W. Sinkovits, G. Pilania, A. R. Oganov, S. Kumar, G. A. Sotzing, S. A. Boggs, and R. Ramprasad, "Rational design of all organic polymer dielectrics," Nat. Commun., Vol. 5, pp. 4845–4852, 2014.
[21] C. C. Wang, G. Pilania, S. A. Boggs, S. Kumar, C. Breneman, and R. Ramprasad, "Computational strategies for polymer dielectrics design," Polymer, Vol. 55, No. 4, pp. 979–988, 2014.
[22] A. Mannodi-Kanakkithodi, G. Pilania, T. D. Huan, T. Lookman, and R. Ramprasad, "Machine learning strategy for accelerated design of polymer dielectrics," Sci. Rep., Vol. 6, p. 20952, 2016.
[23] P. Hohenberg and W. Kohn, "Inhomogeneous electron gas," Phys. Rev. B, Vol. 136, No. 3B, pp. B864–B871, 1973.
[24] G. Kresse and J. Hafner, "Ab initio molecular dynamics for liquid metals," Phys. Rev. B, Vol. 47, No. 1, pp. 558–561, Jan. 1993.
[25] C. C. Wang, G. Pilania, and R. Ramprasad, "Dielectric properties of carbon-, silicon-, and germanium-based polymers: A first-principles study," Phys. Rev. B, Vol. 87, No. 3, p. 35103, 2013.
[26] G. Pilania, C. C. Wang, K. Wu, N. Sukumar, C. Breneman, G. Sotzing, and R. Ramprasad, "New group IV chemical motifs for improved dielectric permittivity of polyethylene," J. Chem. Inf. Model., Vol. 53, No. 4, pp. 879–886, 2013.
[27] A. Mannodi-Kanakkithodi, C. C. Wang, and R. Ramprasad, "Compounds based on group 14 elements: building blocks for advanced insulator dielectrics design," J. Mater. Sci., Vol. 50, No. 2, pp. 801–807, 2014.
[28] T. D. Huan, A. Mannodi-Kanakkithodi, C. Kim, V. Sharma, G. Pilania, and R. Ramprasad, "A polymer dataset for accelerated property prediction and design," Sci. Data, Vol. 3, p. 160012, 2016.
[29] G. Pilania, C. Wang, X. Jiang, S. Rajasekaran, and R. Ramprasad, "Accelerating materials property predictions using machine learning," Sci. Rep., Vol. 3, p. 2810, 2013.
[30] S. Wu, Q. Burlingame, Z.-X. Cheng, M. Lin, and Q. M. Zhang, "Strongly dipolar polythiourea and polyurea dielectrics with high electrical breakdown, low loss, and high electrical energy density," J. Electron. Mater., Vol. 43, No. 12, pp. 4548–4551, 2014.
[31] W. Li, L. Jiang, X. Zhang, Y. Shen, and C. Nan, "High-energy-density dielectric films based on the polyvinylidene fluoride and aromatic polythiourea for capacitors," J. Mater. Chem. A, Vol. 2, No. 38, pp. 15803–15807, Jul. 2014.
[32] Q. Burlingame, S. Wu, M. Lin, and Q. M. Zhang, "Conduction mechanisms and structure-property relationships in high energy density aromatic polythiourea dielectric films," Adv. Energy Mater., Vol. 3, No. 8, pp. 1051–1055, 2013.
[33] S. Wu, W. Li, M. Lin, Q. Burlingame, Q. Chen, A. Payzant, K. Xiao, and Q. M. Zhang, "Aromatic polythiourea dielectrics with ultrahigh breakdown field strength, low dielectric loss, and high electric energy density.," Adv. Mater., Vol. 25, No. 12, pp. 1734–8, 2013.
[34] R. Ma, V. Sharma, A. F. Baldwin, M. Tefferi, I. Offenbach, M. Cakmak, Y. Cao, R. Ramprasad, and G. A. Sotzing, "Rational design and synthesis of polythioureas as capacitor dielectrics," J. Mater. Chem. A, Vol. 3, pp. 14845–14852, 2015.
[35] M. Tefferi, R. Ma, G. Treich, G. Sotzing, R. Ramprasad, and Y. Cao, "Novel dielectric films with high energy density," IEEE Conf. Electr. Insul. Dielectr. Phenomena (CEIDP), pp. 451–454, 2015.
[36] N. G. McCrum, B. E. Read, and G. Williams, *Anelastic and Dielectric Effects in Polymeric Solids,* Dover Publications, 1967.
[37] S. Havriliak and S. Negami, "A complex plane representation of dielectric and mechanical relaxation processes in some polymers," Polymer, Vol. 8, pp. 161–210, 1967.
[38] Y. Sun, S. Boggs, and R. Ramprasad, "The effect of dipole scattering on intrinsic breakdown strength of polymers," IEEE Trans. Dielectr. Electr. Insul., Vol. 22, No. 1, pp. 495–502, 2015.
[39] I. Offenbach and M. Cakmak, "Role of relaxation on strain induced crystallization of uniaxially stretched PI(BTDA-HDA) films: real-time infrared-mechano-optical behavior and electrical study," unpublished.
[40] I. Offenbach and M. Cakmak, "Real-time mechano-optical Behavior and structural evolution of polyimide (BTDA-HDA) during uniaxial deformation," University of Akron, USA, 2015. Unpublished.
[41] A. F. Baldwin, R. Ma, A. Mannodi-Kanakkithodi, T. D. Huan, C. Wang, M. Tefferi, J. E. Marszalek, M. Cakmak, Y. Cao, R. Ramprasad, and G. A. Sotzing, "Poly(dimethyltin glutarate) as a prospective material for high dielectric applications," Adv. Mater., Vol. 27, No. 2, pp. 346–351, 2015.

Gregory M. Treich was born in New Jersey, USA in 1990. He received his Bachelor of Science degree in Chemistry from Rensselaer Polytechnic Institute in 2013 and is currently pursuing a Ph.D. in Polymer Science from the University of Connecticut. His research interests include dielectric materials for capacitor applications, conductive polymers for wearable electronics, and bio-derived materials.

Mattewos Tefferi graduated with a Msc in Electric power engineering from Chalmers University of Technology in 2013. He is currently a PhD candidate in Electrical Insulation Research Center (EIRC), University of Connecticut.

Shamima Nasreen received her Bachelor of Science degree in Chemistry from University of Dhaka, Bangladesh in 2006 and she completed her Masters in inorganic and analytical chemistry in 2008 from the same university. Currently she is perusing her Ph.D. degree in the Polymer Division, from the Department of Chemistry at the University of Connecticut, USA. Her research interest includes metal containing polymers, organic polymers and their dielectric applications

Arun Mannodi-Kanakkithodi was born in India in 1989. He received his Bachelor of Technology degree from the Indian Institute of Technology Roorkee in 2012, and is currently pursuing his Ph.D. degree in materials science and engineering from the University of Connecticut. His research interests include first principles computations, dielectric applications, polymer electronics and machine learning.

Zongze Li was born in Taiyuan Shanxi, China in 1991. He received the B.E. degree from Tongji University, Shanghai, China in 2014, and he is currently a Ph.D. degree student in Department of Electrical and Computer Engineering in University of Connecticut, Storrs, USA. His research is focused on high-field characterization on novel materials for capacitors.

Rampi Ramprasad is presently a Professor of Materials Science and Engineering at the University of Connecticut. His area of expertise is in the development of quantum mechanics and machine learning based computational tools, and in the application of such methods for the design and discovery of new materials, especially functional, electronic, dielectric and catalytic materials.

Gregory A. Sotzing Is presently a Professor of Chemistry at the University of Connecticut. He obtained his Ph.D. degree from the University of Florida under Dr. Reynolds and was a Postdoctoral Fellow at California Institute of Technology under Dr. Grubbs and Dr. Lewis. His research interests include tuning electrochemical polymers, improving the qualities of conductive polymers, and fabricating smart textiles. He also is interested in synthesizing new organic and organometallic polymers for energy storage applications.

Yang Cao was graduated with BS and MS in physics from Tongji University in Shanghai, China, and received his Ph.D. degree from the University of Connecticut in 2002, after which he served as a senior electrical engineer at GE Global Research Center. Since 2013, he has been an associate professor at the Electrical and Computer Engineering Department of the University of Connecticut. His research interests are in the physics of materials under extremely high field and the development of new dielectric materials, particularly the polymeric nanostructured materials, for energy efficient power conversion and renewables integrations, as well as for novel medical diagnostic imaging devices. He can be reached at yang.cao@uconn.edu.